1992

P.A. Zegeling

Moving-finite-element solution of time-dependent partial differential equations in two space dimensions

Department of Numerical Mathematics Report NM-R9206 April

CWI is the research institute of the Stichting Mathematisch Centrum, which was founded on February 11, 1946, as a non-profit institution aiming at the promotion of mathematics, computer science, and their applications. It is sponsored by the Dutch Government through the Netherlands organization for scientific research (NWO).

Moving-Finite-Element Solution of Time-Dependent Partial Differential Equations in Two Space Dimensions

P.A. Zegeling
CWI
P.O. Box 4079, 1009 AB Amsterdam, The Netherlands

The aim of this paper is to show the capability of the 2D moving-finite-element method (MFE) to solve different kinds of time-dependent partial differential equations having solutions with steep moving fronts, rotating pulses, or other features involving fine scale structures. Some difficulties are discussed that can arise, e.g., the treatment of second-order differential operators in combination with MFE. The numerical performance of MFE applied to three model examples, each from a different subclass of PDEs, is studied. Some of the examined aspects are: the efficiency of the temporal integration process, the effect of the regularization parameters (penalties), and the effect of the (PDE-)diffusion coefficient. Further, a more sophisticated application of MFE to a 2D brine transport problem in a porous medium is discussed.

1991 Mathematics subject classification: Primary: 65M60. Secondary: 65M20, 65M50.
Key words & Phrases: Moving finite elements, partial differential equations, time-dependent problems, Lagrangian methods, method of lines.

Note: This paper will be submitted for publication elsewhere.

This work is part of a joint CWI/Shell project on 'Adaptive Grids'. For this project the author has received support from the 'Netherlands Foundation for the Technical Sciences' (STW) (Contract no. CWI 59.0922).

1. INTRODUCTION

The aim of this paper is to show the capability of the 2D moving-finite-element method (MFE) to solve different kinds of time-dependent partial differential equations (PDEs) having solutions with steep moving fronts, rotating pulses, or other features involving fine scale structures. MFE belongs to the class of moving-grid methods, which is a subclass of the class of (time-dependent) adaptive-grid methods. Adaptive-grid methods are numerical methods for PDEs which strive to resolve the sharp transitions in the PDE solution to acceptable degrees of accuracy thereby avoiding the use of an excessive amount of spatial grid points. Fixed-grid methods are in such situations computationally inefficient, since, to afford an accurate approximation, they should contain an unacceptably large number of nodes. Adaptive methods use non-fixed, non-uniform or locally uniform grids and automatically concentrate the grid in regions of high spatial activity during the time-integration process.

In contrast with the one-dimensional case (see, e.g., [20, 24, 34]), application of moving-grid methods in two space dimensions is less trivial. For instance, there are many possiblities to treat the one-dimensional boundary and to discretize the spatial domain each having their own difficulties for specific PDEs. Therefore, 2D moving-grid methods have hardly been applied to real-life problems. The MFE method [10, 14, 20, 24], considering its general approach, allows in principle a large class of PDE problems to be dealt with.

Report NM-R9206
ISSN 0169-0388
CWI
P.O. Box 4079, 1009 AB Amsterdam, The Netherlands

However, because of the intrinsic coupling between the discretization of the PDE and the grid selection, the application of MFE, as for any other method, is not without difficulties. The main difficulty we are referring to is the threat of grid distortion. Grid distortion can occur in many different ways due to the quite complex solution behaviour of 2D-evolution problems [37]. This paper describes some aspects of the MFE method when applied to various kinds of PDEs with different underlying background. More precisely, three main PDE characteristics are recognized, i.e. convection, diffusion, and reaction. For each of this notions MFE acts differently with respect to efficiency (time-integration process), grid movement, etc..

MFE is based on the well-known numerical method-of-lines (MOL) approach for solving time-dependent PDEs. The MFE-method used here restricts its finite-dimensional approximation to a piecewise linear function on a hexagonally connected triangularization of the 2D spatial domain. The grid movement is generated by a least-squares minimization of the so-obtained PDE residual with respect not only to the time-derivatives of the solution amplitudes, as in the standard (fixed-grid) Galerkin case, but also to the now unknown grid velocities. This procedure yields, according to the MOL idea, a large system of stiff ODEs, which may be integrated with a sophisticated implicit stiff ODE/DAE solver, for example the SPGEAR module in the SPRINT package [8, 9].

In literature, several tests of the MFE method in 2D are described. These can be found, e.g. in [3, 6, 10, 14, 18, 29, 37]. Theoretically, however, little is known about the moving-finite-element method in 2D. An exception in this respect is the work by Baines and Wathen [4, 7, 35, 36], and Miller [23]. A very important theoretical property is the relation of MFE in both 1D and 2D, for hyperbolic PDEs, with the method of characteristics [4]. Secondly, for convection/diffusion equations with a small diffusion coefficient it can be shown that MFE resembles a perturbed method of characteristics [4,37]. Additionally, in the case of parabolic equations there is a strong link of MFE with equidistribution principles [37]. All these properties have their influence on the performance of the method when applied to different types of PDEs, as we will see in this paper.

The paper is divided into four sections. In Section 2.1 we describe the MFE method for a general system of PDEs in two space dimensions. The treatment of second-order operators is discussed in Section 2.2. Section 3.1 shows an application of MFE to convection-reaction equations. A special feature of this section is the use of a non-rectangular domain for the so-called 'Molenkamp-test' (see also [26, 30]), which is an important testproblem in meteorology. In Section 3.2 MFE is applied to a reaction-diffusion equation from combustion theory [19, 27]. An interesting aspect in this section is the effect of the regularization parameters (penalties) on the grid movement, quality of the solution, and the numerical time-stepping procedure, respectively. Section 3.3 deals with convection-diffusion equations, and shows the effect of a small diffusion coefficient in the PDE on the semi-discrete MFE system. Also in this section, MFE is applied to a system of nonlinear brine transport problems in a porous medium, of importance in the field of hydrology [33, 38]. Finally, Section 4 is devoted to some concluding remarks.

2. Description of MFE in two space dimensions

2.1. The method

In this section a description is given of the moving-finite-element method in two space dimensions. For more details the reader is referred to [10, 11, 20, 24]. The method is presented along the lines of the numerical method-of-lines (MOL) approach.

Consider an abstract Cauchy problem for a system of PDEs in two space dimensions,

$$\frac{\partial u^{(j)}}{\partial t} = L_j, \qquad j=1, \cdots, p \qquad (x,y)\in\Omega, \ t>0, \tag{2.1}$$

where L_j is a spatial differential operator containing at most second-order derivatives. The MFE-approximation to $u^{(j)}$ is chosen to be piecewise linear on a hexagonally connected triangularization of Ω

$$u^{(j)} \approx U^{(j)} = \sum_{l=1}^{M} U_l^{(j)}(t)\, \alpha_l(x,y,\{X_l(t),Y_l(t)\}), \qquad j=1, \cdots, p, \tag{2.2}$$

where M denotes the total number of gridpoints, and α_l are the standard piecewise linear hat functions. Differentiating (2.2) with respect to t by the chain rule, and using the time-dependence of the gridpoints $(X_l(t), Y_l(t))$ we obtain

$$U_l^{(j)} = \sum_{l=1}^{M} \dot{U}_l^{(j)} \alpha_l + \dot{X}_l \beta_l^{(j)} + \dot{Y}_l \gamma_l^{(j)}, \qquad j=1, \cdots, p. \tag{2.3}$$

The basis functions $\beta_l^{(j)}$ (see Figure 2.1) have the same support as α_l, i.e. the hexagon of triangles surrounding the j-th node. They are discontinuous at the center and on the inner edges of the hexagon; they are zero on the hexagonal boundary and take on (for each PDE-component) the six different values of $-\partial U^{(l)}/\partial x$ at the central vertices of the six triangles. Note that due to the piecewise linear approximation (2.2), $-\partial U^{(l)}/\partial x$ has a constant value on each triangle. A similar description holds for $\gamma_l^{(j)}$, but now related to $-\partial U^{(l)}/\partial y$.

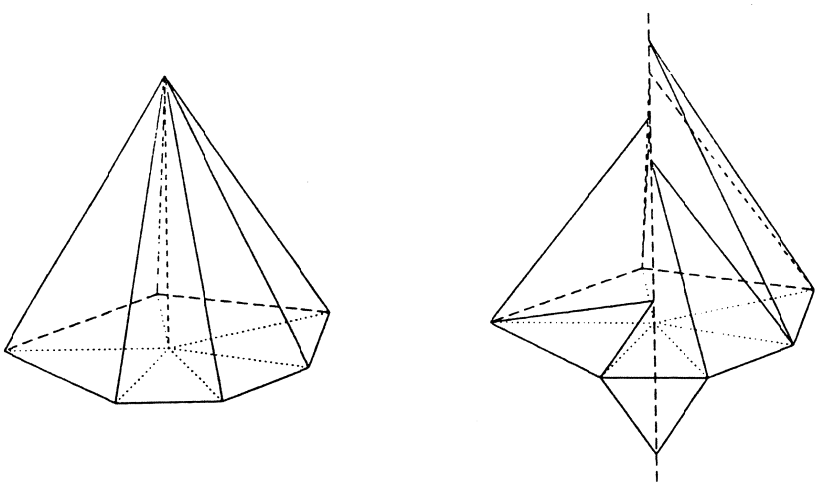

FIGURE 2.1. The basis functions α_l (left) and $\beta_l^{(j)}$ (right).

The equations determining the semi-discrete unknowns $U_l^{(j)}$, X_l and Y_l are now obtained in the standard Galerkin way by minimizing the PDE residual R with respect to $U_i^{(j)}$, $\dot{X}_i$ and $\dot{Y}_i$, where

$$R := \sum_{j=1}^{p} w_j \, \|U_l^{(j)} - L_j(U)\|^2_{L_2(\Omega)} + \sum_l P_l^2. \tag{2.4}$$

Here w_j are non-negative weight factors and P_l is the grid-regularization term (penalty) (see [11])

$$P_l := e_l \dot{\Delta}_l - S_l, \tag{2.5a}$$

with

$$e_l^2 := \frac{\varepsilon_1^2}{\Delta_l}, \tag{2.5b}$$

and

$$e_l S_l := \left(\frac{\varepsilon_2}{\Delta_l}\right)^2, \tag{2.5c}$$

where ε_1^2 and ε_2^2 are small user-specified constants. The effects of adding this penalty term are explained below. Note that the second sum in (2.4) is taken over the three perpendiculars Δ_l of each triangle. The

minimization of (2.4) is performed by setting

$$\frac{\partial R}{\partial \dot{U}_i^{(j)}} = 0, \quad \text{for } i=1,\cdots,M;\ j=1,\cdots,p,$$

$$\frac{\partial R}{\partial \dot{X}_i} = \frac{\partial R}{\partial \dot{Y}_i} = 0, \quad \text{for } i=1,\cdots,M$$

and results in a large system of $(p+2)\times M$ ordinary differential equations in the unknowns $U_i^{(j)}$, X_i and Y_i:

$$\sum_{l=1}^{M} <\alpha_i,\alpha_l>\dot{U}_l^{(j)} + <\alpha_i,\beta_l^{(j)}>\dot{X}_l + <\alpha_i,\gamma_l^{(j)}>\dot{Y}_l = <\alpha_i,L_j(U)>, \tag{2.6a}$$

$$\text{for } i=1,\cdots,M;\ j=1,\cdots,p,$$

$$\sum_{j=1}^{p} w_j \sum_{l=1}^{M} <\beta_i^{(j)},\alpha_l>\dot{U}_l^{(j)} + <\beta_i^{(j)},\beta_l^{(j)}>\dot{X}_l + <\beta_i^{(j)},\gamma_l^{(j)}>\dot{Y}_l + \sum_l P_l \frac{\partial P_l}{\partial \dot{X}_i} = \sum_{j=1}^{p} w_j <\beta_i^{(j)},L_j(U)>, \tag{2.6b}$$

$$\text{for } i=1,\cdots,M,$$

$$\sum_{j=1}^{p} w_j \sum_{l=1}^{M} <\gamma_i^{(j)},\alpha_l>\dot{U}_l^{(j)} + <\gamma_i^{(j)},\beta_l^{(j)}>\dot{X}_l + <\gamma_i^{(j)},\gamma_l^{(j)}>\dot{Y}_l + \sum_l P_l \frac{\partial P_l}{\partial \dot{Y}_i} = \sum_{j=1}^{p} w_j <\gamma_i^{(j)},L_j(U)>, \tag{2.6c}$$

$$\text{for } i=1,\cdots,M,$$

where $<.,.>$ denotes the usual L_2-innerproduct. It is clear that (2.6a) without the $\dot{X}$- and $\dot{Y}$-innerproducts is just the standard Galerkin method applied to (2.1) using piecewise linear basis and trial functions on a nonuniform triangular grid. The time-dependency of the grid is reflected in the $\dot{X}$- and $\dot{Y}$-innerproducts in (2.6a) and the complete equations (2.6b) and (2.6c).

Working out the innerproducts and defining the vector

$$\eta := (\cdots, U_i^{(1)}, \ldots, U_i^{(p)}, X_i, Y_i, \cdots)^T,$$

we arrive at the semi-discrete MFE system

$$A(\eta,\varepsilon_1^2)\,\dot{\eta} = G(\eta,\varepsilon_2^2), \quad t>0, \quad \eta(0) \text{ given}, \tag{2.7}$$

where A is a symmetric matrix, the so-called mass-matrix, containing quantities from the left-hand sides of (2.6), whereas the only problem-specific terms are contained in the vector G. It must be noted that, for $\varepsilon_1=\varepsilon_2=0$, i.e. without regularization terms, there exist fundamental difficulties with solving system (2.7).

The first difficulty is a possible singularity in the mass-matrix A. The matrix A is singular in the so-called case of 'parallelism'. Parallelism occurs in the absence of curvature in the solution of the PDE. In this case, the basisfunctions $\beta_i^{(j)}$ and α_i (and/or $\gamma_i^{(j)}$ and α_i) become linearly dependent, which means that the parametrization of the time-derivative $U_i^{(j)}$ in (2.3) degenerates. In other words, the minimization procedure then has no unique solution, resulting in a zero mass-determinant: $\det A(\eta,0)=0$. Therefore, to avoid the problem of solving a DAE system of index 1 or higher, the ε_1^2-term (2.5b), also called intratriangular viscosity, was introduced in the residual (2.4). It can be shown, that, for $\varepsilon_1\neq 0$, A is positive-definite and thus regular. The second degeneracy of A arises whenever the triangles get too thin or lose their positive orientation, i.e. '2D mesh-tangling'. The matrix A will then become very ill-conditioned and numerically singular, because in such cases the triangle area tends to zero, giving widely varying eigenvalues. Note, that this behaviour is time-dependent. Both singularities of the mass-matrix are also discussed theoretically in [36]. Since it appears in the left-hand side of (2.7), the parameter ε_1 can also be seen to serve as a tool to control the grid-point motion.

Another difficulty in (2.7) could arise from a possible singularity of the nonlinear steady-state system: $G(\eta,0)=0$. In the already described case of parallelism, which appears in applications with, e.g. a constant steady-state, the system $G=0$ could have non-unique solutions. The parameter ε_2 in (2.5c) ('intratriangular spring force') serves to prevent this degeneracy.

As for any other method, the regularization is somewhat heuristic and necessarily problem-dependent. For example, if ε_1 is chosen too large, the grid movement is restricted; $\varepsilon_1 \to \infty$ gives a non-moving grid, with the result that there may not be sufficient refinement in regions of large spatial activity. On the other hand, if ε_1 is too small, the mass-matrix A may become numerically singular. The parameter ε_2 could be chosen equal to zero in most applications. For PDEs with 'flat' steady-state solutions a small non-zero value of ε_2 suffices to keep the semi-discrete ODE system regular. As for ε_1, too large values for ε_2 could restrict the grid movement: $\varepsilon_2 \to \infty$ gives a uniform (non-moving) grid.

The weight-factors w_j in (2.4) serve to make it possible to let certain PDE components dominate the grid movement equations (2.6b) and (2.6c). This may be desirable for a badly scaled problem, or if one PDE component is strongly varying and a second component has only a mildly varying solution, for example.

2.2. Second-order operators

The MFE method used here has serious difficulties, when solving PDEs with second derivative terms. Due to the piecewise linear approximation (2.2), second order derivatives fail to be defined in the usual sense. For example, Δu is zero on the interior of each triangle, but makes non-zero jumps over the inner edges of a triangle. Furthermore, the basis function β_i has a discontinuity along each inner edge. This can be derived from the relation $\beta_i = -U_x \alpha_i$. These two properties combined make it impossible to evaluate the innerproduct $<\beta_i, \Delta u>$ without regularization. Note that these considerations hold for the right-hand side γ-innerproducts in (2.6c) as well.

There are several 'tricks' to get around this fundamental difficulty:

1. Miller [20, 24] uses the idea of 'mollification' to regularize the undefined innerproducts. Mollification can be interpreted as using a limiting equation obtained by applying the minimizing condition to a PDE residual underlying a smoothed (mollified) piecewise linear function and then letting the limiting equation approach its now well-defined limit (using a small perturbation parameter, the so-called δ-mollifier).
2. Johnson [17] and Mueller [28] apply Green's theorem in a clever way to work out the troublesome innerproducts. Their treatment, however, can only be used for special PDE operators.
3. Sweby [31] uses the idea of 'recovery'. This involves fitting a piecewise polynomial to the first derivative and then differentiating this better defined quantity. The process is simple in one dimension, but in two dimensions the expressions may become very complex.
4. Higher order test functions. This means, that instead of applying a minimization of the PDE residual, we do a projection on a higher order function space. Then, no problems are encountered when evaluating the right-hand side innerproducts. This Petrov-Galerkin approach works well in 1D (see [16]), and seems to improve the nodal movement and position of the grid points in steep fronts. In 2D, however, the evaluation of the innerproducts is not so simple and straightforward as in one space dimension.

It is interesting to note, that for the relatively simple case of a Laplacian operator ideas 1. and 2. yield identical semi-discrete equations. This is expressed by the following Lemma:

LEMMA 2.1 The right-hand side innerproducts in (2.6b) for $L(u) = \Delta u$ using mollification are identical to the ones using idea 2. In other words:

$$<\beta_i, \Delta u>_{1.} = <\beta_i, \Delta u>_{2.}. \tag{2.8}$$

PROOF By definition we have:

$$<\beta_i, \Delta u>_{2.} = \int_\Omega \beta_i u_{xx}\, d\Omega + \int_\Omega \beta_i u_{yy}\, d\Omega = -\int_{6\tau} u_x \alpha_i u_{xx}\, d\Omega - \int_{6\tau} u_x \alpha_i u_{yy}\, d\Omega,$$

where 6τ are the six triangles surrounding the grid point (X_i, Y_i). Applying the chain rule, the divergence theorem, and the small support of α_i, respectively, this expression can be written as

$$\sum_{6\tau} \left(\frac{1}{2}\alpha_{i,x}(\tau)(u_x^2(\tau) - u_y^2(\tau))\, A(\tau) + \alpha_{i,y} u_x(\tau) u_y(\tau)\, A(\tau)\right), \tag{2.8a}$$

where $A(\tau)$ is the area of triangle τ. Next, using relations between $\alpha_{i,x}$, $\alpha_{i,y}$, $A(\tau)$, the lengths L of an edge, and the unit normal vector n on an edge, (2.8a) can be rewritten as

$$\sum_{6\tau} \sum_{2\ i.e.} [(n_1(\frac{\partial u}{\partial n})^2 - 2n_2 \frac{\partial u}{\partial n}\frac{\partial u}{\partial \tau})\frac{L}{4}] \qquad (i.e. = \text{inner edge}),$$

where n_1 and n_2 denote the x- and y-component of the normal vector n, $\frac{\partial u}{\partial n}$ the normal and $\frac{\partial u}{\partial \tau}$ the tangential derivative on each edge, and the second sum is taken over the two inner edges of τ. Expressing $\frac{\partial u}{\partial n}$ and $\frac{\partial u}{\partial \tau}$ in terms of u_x, u_y and n, finally results in

$$\sum_{6\ edges} (\frac{\partial u^+}{\partial n} + \frac{\partial u^-}{\partial n})\frac{u_x^+ + u_x^-}{2}\frac{L}{2}.$$

This is equal to $<\beta_i, \Delta u>_{1,}$, since the mollified form consists of $-(\frac{\partial u^+}{\partial n} + \frac{\partial u^-}{\partial n})$ (the constant measure of Δu on each inner edge) and $-\frac{u_x^+ + u_x^-}{2}$, which can be interpreted as a mean value for $-u_x$ along an edge (see [11]). □

To apply MFE to real-life problems, such as the brine transport problem in Section 3.4, involves the treatment of a general second order flux term in combination with the piecewise discontinuous basis functions β_i and γ_i. In this case, option 2. can not be used, and options 1. and 3. yield extremely complicated nonlinear semi-discrete terms in the right-hand side vector G in equation (2.7). We have used another idea, which is in our opinion the simplest justifiable option. The idea makes use of the fact, that, owing to the piecewise linear approximation, the first order spatial derivatives are constant on each triangle. For instance, the innerproduct of β_i with a flux term $\nabla\cdot\phi(u,\nabla u)$ is treated as follows:

$$<\beta_i, \nabla\cdot\phi(u,\nabla u)> := \int_\Omega \beta_i\, \nabla\cdot\phi(u,\nabla u)\, d\Omega = \int_{6\tau} -U_x\, \alpha_i\, \nabla\cdot\phi(u,\nabla u)\, d\Omega$$

$$\approx \sum_{6\tau} -U_x(\tau) \int_\tau \alpha_i\, \nabla\cdot\phi(u,\nabla u)\, d\tau, \qquad (2.9)$$

where the last integral may be approximated without difficulties in the usual way by some quadrature rule, e.g. the mid-point rule. It must be noted, that using (2.9) is a bit tricky, because the jumps of β_i-values over triangle edges are, more or less, averaged in the approximating integral. In some sense, when replacing ϕ by ∇u, giving back the Laplacian, (2.9) is an averaged approximation to formulas (2.8). Moreover, 'freezing' one space dimension in (2.9), say the y co-ordinate, approximates the mollified interpretation of $<\beta_i, u_{xx}>$, viz., applying (2.9) to $<\beta_i, u_{xx}>$ yields:

$$<\beta_i, u_{xx}> = \int_{X_{i-1}}^{X_{i+1}} -u_x \alpha_i u_{xx}\, dx \approx \sum_{2el} -U_{x,el} \int_{el} \alpha_i u_{xx}\, dx \approx -\bar{U}_{x,2el} \sum_{2el} \int_{el} \alpha_i u_{xx}\, dx \quad (el = \text{element}),$$

where $\bar{U}_{x,2el}$ is the average value of U_x over the two elements. Defining m_i to be U_x on the element (X_{i-1}, X_i) and working out the integral by partial integration, we obtain

$$-\frac{m_i + m_{i+1}}{2}(m_{i+1} - m_i) = -\frac{1}{2}(m_{i+1}^2 - m_i^2).$$

The last expression is equivalent to $<\beta_i, u_{xx}>_1$. (see [24]).

For the brine-transport application, we evaluate the flux innerproducts according to the idea above. In the other numerical experiments in this paper the second idea is used for the Laplacian-innerproducts.

3. AN EVALUATION OF MFE IN 2D

We implemented system (2.6) according to [11]. This holds also for the treatment of the boundary terms. To obtain the fully discretized solution, ODE system (2.7) must be integrated numerically. It is known, that this system will usually be extremely stiff. For integration in time, therefore, a suitable stiff ODE solver must be used. In our numerical experiments we have solved the implicit ODE system (2.7) with the (implicit) BDF integrator SPGEAR of the SPRINT package [8, 9] in the usual way. This means amongst others that the resulting algebraic system is solved by a modified Newton process. In the description of the experiments, which all were done on an SGI Indigo workstation, the following notation is used:

STEPS = number of successful time-integration steps
JACS = number of Jacobian evaluations
BS = total number of Newton iterations
TOL = time-tolerance (absolute and relative) for the SPGEAR integrator

3.1. Application to convection-reaction equations

For this type of PDEs a standard form for the right-hand side operator L in (2.1) is

$$L(u) = -\gamma \cdot \nabla u + g(u,x,y,t), \tag{3.1}$$

where γ defines the convection term, and may depend on u, x, y, and t. This means, that (2.1) for this choice of L is of the hyperbolic type. MFE applications to this class of PDEs can be found in [3, 6, 28, 29, 37]. It is known, see e.g. [4], that, for this choice of PDE operator, there is a strong link between the semi-discrete MFE system (without regularization terms) and the characteristic equations of the PDE. More specifically, it can be shown that for PDE operators L of the form (3.1) with γ linear in u, x, y, while setting aside boundary effects, the ODE system (2.7) is equivalent to a discretized version of

$$(\dot{x}, \dot{y})^T = \gamma, \tag{3.2a}$$

$$\dot{u} = g. \tag{3.2b}$$

In many cases, this characteristic behaviour is very beneficial. However, there are some situations in 2D for which this behaviour could give problems. Two of these problems are described in [37]. The first problem has to do with a possible difference between the directions of the characteristic curves of the PDE (the movement of the 'fluid'-particles) and the movement of the solution front. The second problem can be summarized by the term 'grid rotation', and may occur in PDE problems where the characteristic curves are circles, spirals, etc. Furthermore, equations (3.2) show, that for γ=0, i.e. when we are dealing with an ODE instead of a PDE, there will be no grid movement at all. This is a desirable property, since pure ODEs can not produce propagating wave solutions.

The following numerical example from this PDE class is the so-called 'Molenkamp-test', which is a standard test problem in meteorology (see also [25, 26, 30]). In fact, this example is identical to Example II in [37] enhanced with a linear reaction term. It was this example (without reaction term) for which MFE produced a strongly distorted grid when applied on a square with fixed corner points. It will be shown that, if we let the boundary points 'move around the corner', MFE produces a very accurate solution on a well-adapted grid. The effect on MFE of adding the reaction term will be examined as well.

EXAMPLE I ('Molenkamp-test'):

The operator L reads for this test-problem:

$$L(u) = -\pi\,(y-\frac{1}{2})\frac{\partial u}{\partial x} + \pi\,(x-\frac{1}{2})\frac{\partial u}{\partial y} - c\,u, \tag{3.3}$$

with initial and boundary conditions

# rotations	STEPS	JACS	BS	Umax
1	100	68	374	1.00000
3	205	162	842	1.00000
5	289	234	1205	0.99989
7	390	323	1664	0.99989

TABLE 3.1 Example I: Integration history for c=0.

$$u\,|_{t=0} = u_0(x,y) = \exp(-80[(x-\frac{1}{2})^2+(y-\frac{3}{4})^2]),$$

$$u\,|_{\partial\Omega}=0.$$

The domain Ω is chosen to be a circle with center (1/2,1/2) and radius $\sqrt{2}$, in contrast with the experiments in [37], where Ω was represented by a square. It must be noted that the choice of a circular domain is certainly not restrictive. Equation (2.6a) is there replaced by u = 0, whereas equations (2.6b) and (2.6c) are only calculated on the interior of the domain Ω. In fact, the grid points on the boundary are now free to move.

The exact solution describes a pulse that moves around in circles with a constant speed. During the movement the shape of the pulse changes, depending on the value of c in the reaction term. For c=0, the shape of the pulse is unchanged, whereas, for c>0, the peak of the pulse will decrease. The characteristic curves are circles with centre $(\frac{1}{2},\frac{1}{2})$

$$(x-\frac{1}{2})^2+(y-\frac{1}{2})^2 = r^2,\quad 0<r<\sqrt{2}.$$

On these curves the solution varies according to $\dot{u} = -c\,u$, resulting in the exact solution: $u(x,y,t) = u_0\,e^{-c\,t}$.

From literature it is known, that many numerical methods have severe problems with solving this test example (see [25, 30]). Two important drawbacks of standard numerical techniques to solve (3.3) are, that either they damp out the solutions dramatically, because of numerical diffusion, and/or they exhibit strong oscillations in the solution during the integration process.

In Table 3.1 and Figure 3.1 the results for MFE applied to model (3.2) on a circular domain with c=0 are given. In the below described runs the standard choices TOL=1.E-3, ε_1^2=1.E-4 and ε_2^2=1.E-9 are made. In this example the effects of the penalty terms are not essential; they are only needed to keep the semi-discrete system (2.7) non-degenerate. The starting grid consists of only 11×11 points of which 5×5 are distributed uniformly around the cone in (0.25,0.75)×(0.5,1.0).

A notable point is that the integration costs remain almost constant during each rotation of the pulse. This can be explained by the property of MFE to follow the characteristic curves of the PDE, thereby yielding almost linearly (in x and y) varying grid speeds during the calculations. Note, that this is the optimal way to follow the rotating pulse. Also, the maximum value of the pulse shows no tendency to decrease as for other methods. In fact, the error in the peak of the pulse is less than 1.E-4 even after several rotation periods. Both effects can be explained by referring to equation (3.2) with g=0. In contrast with [37], the grid structure now remains undistorted and well-adapted to the shape of the pulse.

If we take a non-zero reaction term, for instance c=1 or c=10 in (3.2), the results do not change dramatically. As for the previous case, the error induced by MFE for the maximum amplitude is less than 1.E-4 for both c=1 and c=10. The time-integration costs are, say for c=1: $STEPS$ = 95, $JACS$ = 68, BS = 361 for the time-period $0 \le t \le 2$. Again, this could be explained by the fact that the semi-discrete MFE system (2.7) is strongly related with equations (3.2), but now with $g \neq 0$.

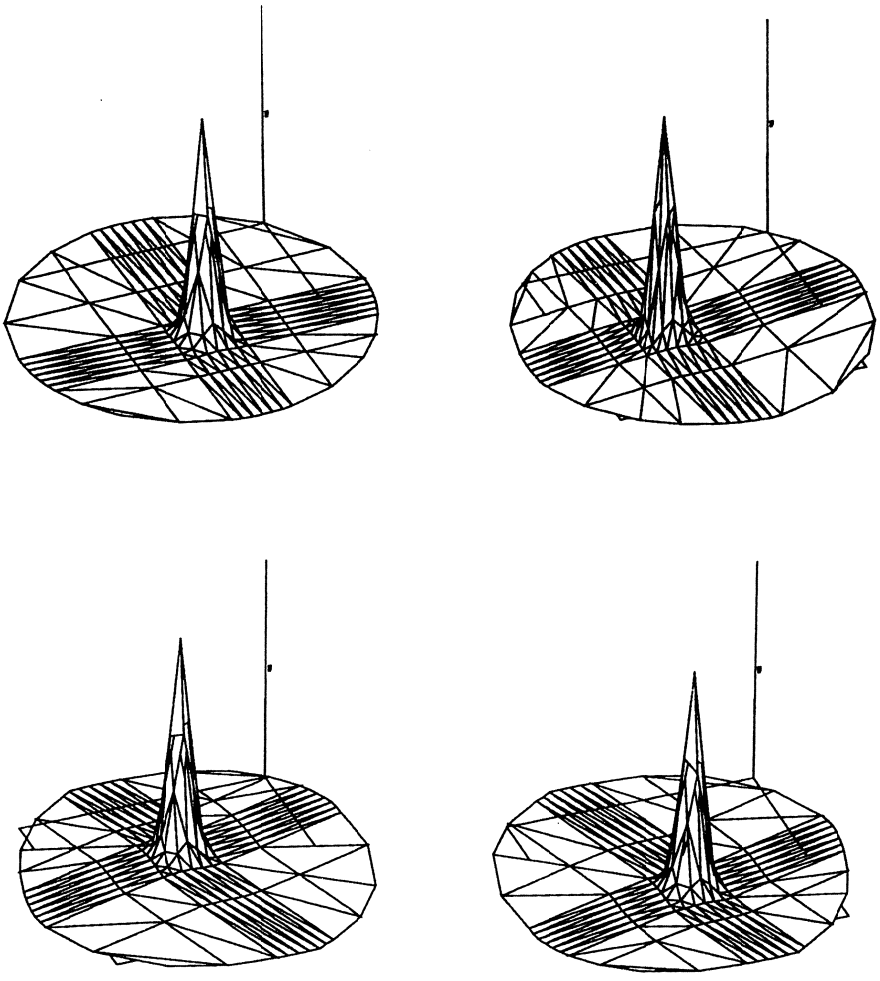

FIGURE 3.1. MFE solution for Example I (c =0) at t= 0.0, 0.5, 1.0 and 2.0.

3.2. Application to reaction-diffusion equations

For this type of PDEs a standard form for the right-hand side operator L in (2.1) is

$$L(u) = \nabla\cdot(D(u)\nabla u) + f(u,x,y,t), \tag{3.4}$$

with a diffusion coefficient D. MFE applications to this class of PDEs can be found in [2, 10, 17, 18, 37].

In the following numerical example, MFE is applied to a scalar reaction-diffusion equation. The effect of the penalty parameters ε_1 and ε_2 on the time-stepping process, the movement of the grid, and the quality of the solution, are examined, respectively.

EXAMPLE II ('Flame propagation'):

This example of the reaction-diffusion type is a model of a so-called single one-step reaction of a mixture of two chemicals [19] and stems from combustion theory. The right-hand side operator L in (2.1) reads in this case

$$L(u) = d\,\Delta u + D(1+a-u)e^{-\delta/u}, \tag{3.5}$$

on the domain $\Omega = (0,1)\times(0,1)$, subjected to the initial and boundary conditions

$$u\,|_{t=0}=1,$$

$$\frac{\partial u}{\partial n}=0, \text{ at } x=0,\ y=0, \quad u=1, \text{ at } x=1,\ y=1.$$

The dependent variable u here represents the temperature of the mixture. The parameter a is the heat release, $D=Re^{\delta}/a\delta$ the Damkohler number, δ the activation energy, and R is the reaction rate. For small times the temperature gradually increases in a circular area around the origin. Then, provided the reaction rate is large enough, at a finite time 'ignition' occurs causing the temperature to suddenly jump from near unity to $1+a$, while simultaneously a reaction front is formed which circularly propagates towards the outer Dirichlet boundary. When the front reaches the boundary the problem runs into steady-state. Following [1] we select the parameter values $a=1$, $\delta=20$, $R=5$, but choose a different value for the diffusion parameter d. While in [1] the diffusion coefficient $d=1$, we have here put $d=0.1$ as in [32]. A smaller diffusion parameter has the effect that the temperature front becomes steeper, particularly so upon approaching steady-state. With this choice of parameters the 'ignition' takes place at about $t=.24$ and the solution is in 'steady-state' at about $t=.35$. It is known (see, e.g., [13] for the one-dimensional case), that BDF codes need a rather small time tolerance *TOL* of, say $1.E-5$, because of the different time-scales in the model. This is especially so to detect the start of ignition accurately. Small errors at this time point result in significantly larger global errors later on. This 'local instability' of the model can be explained by inspection of the reaction term: for $1\le u\le 1.8$ its derivative $\partial f/\partial u$ is positive, for example $1.E+3$ for $u\approx 1.6$, resulting locally in growing solutions and for $u\ge 1.8$ negative, for example $-5.5E+3$ for $u\approx 2.0$, resulting in locally decreasing solutions, respectively.

Since the initial solution is constant, we let MFE start on a uniform grid consisting of 21×21 moving grid points. The experiments shown below are separated in two different subcases. First, a standard value for ε_2^2 is chosen, viz. $1.E-9$, while varying the first penalty parameter ε_1^2 from $1.E-6$ to 1. Second, with a fixed value for ε_1^2, viz. $1.E-4$, the effects of varying ε_2^2 within a range from 0 to 1 are studied.

Figure 3.2 shows the grid and solution generated by MFE at some interesting points of time for the standard choice of parameters $\varepsilon_1^2=1.E-4$ and $\varepsilon_2^2=1.E-9$. Although there is no exact solution available, the numerical solution may be compared with a 'reference' solution obtained by [32], where an adaptive grid with local refinement is used. Both solutions resemble very well, and both adaptive grids, although underlying totally different adaptation principles, indeed generate refinements in the same regions. Moreover, just as in Example III of [37], we see for this PDE (especially in steady-state, i.e. at $t=0.35$) a concentration of triangles in regions with large second derivatives. This corroborates the conjecture that for parabolic equations in 2D there is a close relation between MFE and equidistribution principles. This is, unfortunately, only an experimental evidence, in contrast with the one-dimensional situation for which there is some theory available in this respect.

Tables 3.2 and 3.3 show integration data for increasing values of ε_1^2 and ε_2^2, respectively. From Table 3.2 we note that the efficiency of MFE depends highly on the choice of ε_1. For very small values of this parameter the solution is still accurate, but is computed on a grid which moves not very smoothly in time. We also see, that for larger values of ε_1, the adaptivity of the method is influenced, while for too large choices the grid doesn't move at all. In this respect, the parameter ε_1, originally introduced in the minimization procedure to ensure the regularity of the mass-matrix, can also be seen as a smoothing parameter for the grid movement. The integration performance of MFE is in one aspect disappointing. If we calculate the ratio *JACS/STEPS* as a function of ε_1, we see from the table that for $\varepsilon_1=1.E-4$ this ratio is 0.34, i.e. when using MFE optimally, whereas for $\varepsilon_1=1$ (a fixed grid) *JACS/STEPS* is only 0.12. We may conclude, that the

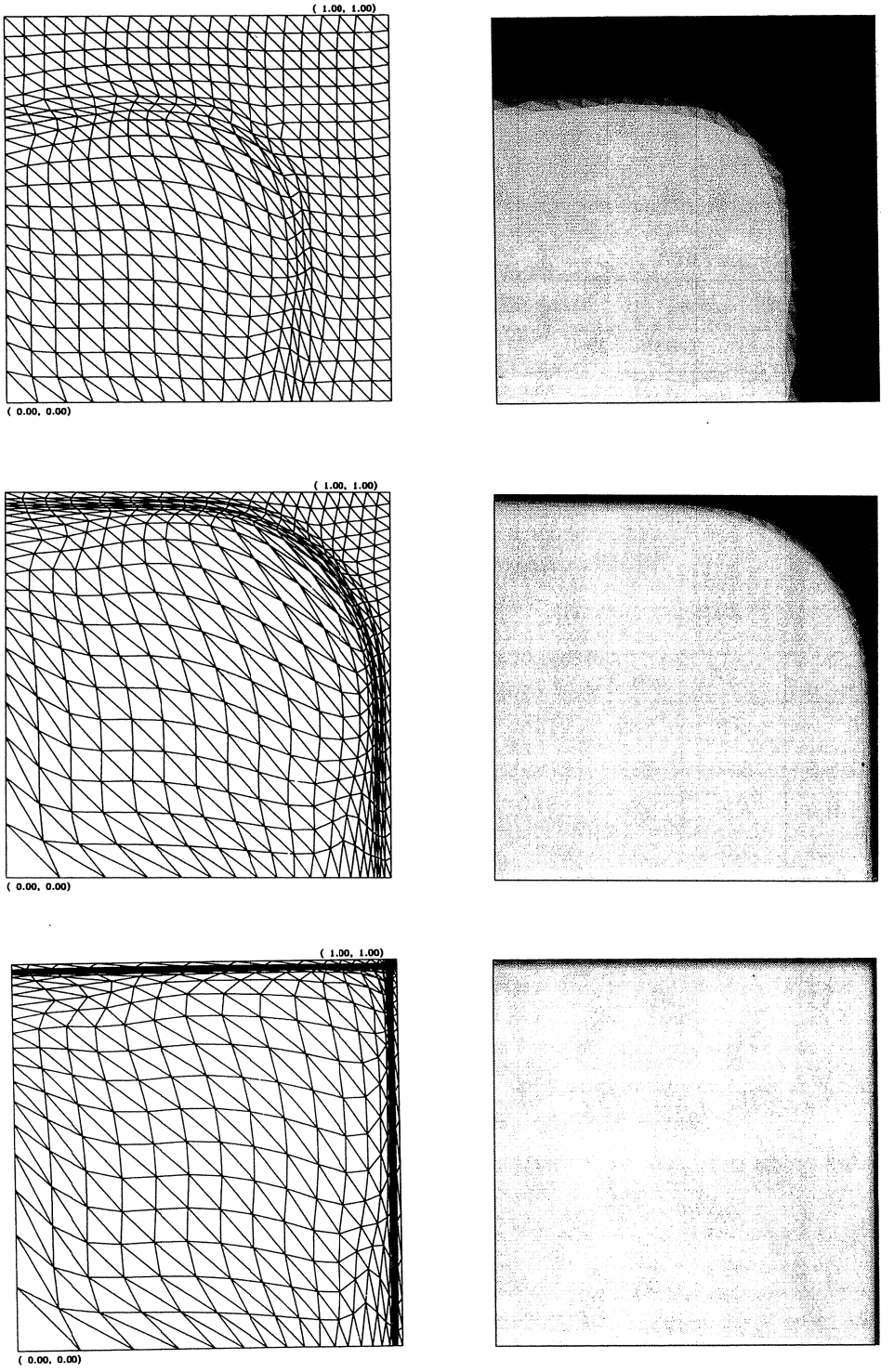

FIGURE 3.2. Grids and solutions of Example II at $t = 0.25237, 0.27653, 0.35000$.

efficiency of MFE, at least for this testproblem, although resulting in accurate solutions, is strongly influenced by the choice of the intratriangular viscosity constant. The effect of the parameter ε_2, introduced to keep the steady-state MFE system regular, is less important (see Table 3.3). In fact, ε_2 could have been chosen equal to zero for this example, since the steady-state solution still possesses a steep profile. Also, the time-integration process is not much influenced by this parameter, in contrast with the penalty constant ε_1. This can be seen in the second column of Table 3.3, where the number of time steps is almost constant for the smaller values of this parameter. Note, that a fixed (uniform) grid, with an inaccurate solution, is obtained, if we let ε_2 tend to infinity. In the case of a flat steady-state, as in the next numerical example, this so-called spring constant plays a more significant role.

ε_1^2	*STEPS*	*JACS*	*BS*	*SOLUTION*(*)	*GRID*(**)
1.E-6	1984	579	5928	O.K.	NON-SMOOTH
1.E-4	618	209	2188	O.K.	ADAPTIVE
1.E-2	502	93	1370	O.K.	TOO SLOW
1.E-0	423	52	1066	BAD	FIXED

TABLE 3.2 Example II: Variation of ε_1^2.
(*): compared with the solution in [32]
(**): this is, of course, a subjective notion

ε_2^2	*STEPS*	*JACS*	*BS*	*SOLUTION*	*GRID*
0	609	188	2105	O.K.	ADAPTIVE
1.E-9	618	209	2188	O.K.	ADAPTIVE
1.E-6	635	186	2212	O.K.	LESS NON-UNIFORM
1.E-3	783	255	2839	INACCURATE	ALMOST UNIFORM
1.E-0	469	75	1250	BAD	UNIFORM

TABLE 3.3 Example II: Variation of ε_2^2.

3.3. Application to convection-diffusion equations

For this type of PDEs a standard form for the righthand-side operator L in (2.1) is

$$L(u) = \varepsilon \Delta u - \beta \cdot \nabla u, \tag{3.6}$$

where, in general, ε is a small coefficient, and β a linear or nonlinear function of u. Depending on the proportion ε/β, the PDE defined by (3.6) can be classified numerically as hyperbolic or parabolic. The numerical difficulties for this type of PDEs, in fact, arise because of this 'double' property: for $\varepsilon \downarrow 0$ the PDE will be of the hyperbolic type, whereas otherwise the PDE will possess parabolic properties. MFE test results for this class of PDEs can be found in [10, 14, 21, 22, 28, 29, 37]. Since the displacement of solution fronts for this type of equations is mainly determined by the convection term $\beta \cdot \nabla u$, the complete movement may be defined by a perturbed characteristic ODE system. In formulas:

$$\dot{\mathbf{r}} = \beta + \varepsilon \mathbf{f}, \quad \dot{u} = \varepsilon h, \quad 0 < \varepsilon \ll 1, \tag{3.7}$$

where $\mathbf{r}$ represents the position vector $(x,y)^T$, and $\mathbf{f}$, h are some functions containing first and second order spatial derivatives of the solution u. Similar to the pure convective case (see Section 3.1), the semi-discrete MFE equations are now related to equations (3.7), of course without penalty terms ($\varepsilon_1=\varepsilon_2=0$). In one space dimension, we can formulate the function $\mathbf{f}$ explicitly, both in the continuous and semi-discrete case, see, e.g., [12, 37]. In [4] it is shown that, in two dimensions, the MFE grid speeds are, in a certain sense, approximations to

$$\dot{\mathbf{r}} = \beta + \varepsilon\,((\Delta u)_x/u_{xx},(\Delta u)_y/u_{yy})^T.$$

It is clear, that the perturbation term $\mathbf{f}$, though multiplied by the small diffusion coefficient ε, may be of importance in subregions of the spatial domain Ω, where the solution of the PDE model possesses large first and second order derivatives, such as in boundary layers and steep transitions. Therefore, a proper treatment of the Laplacian-innerproducts in (2.7) is indispensable.

The following two numerical PDE examples will show the performance of MFE for convection-diffusion equations. First, a simple linear PDE is discussed with the accent on the effects of the semi-discrete diffusion term, especially its effect in a boundary layer and for steady-state situations. The second example is a strongly nonlinear system of two PDEs, describing brine transport in a porous medium. Here, the weightfactors w_j, which were defined in (2.4), play an important role. An additional aspect in this example is the use of general second order flux terms.

EXAMPLE III ('A linear model'):

For this example we have chosen the convection term β to be constant: $\beta = (\beta_1,\beta_2)^T = (1,1/2)^T$, and two different values for ε: $1.E-2$ and $1.E-3$. The domain Ω is the unit square and the boundary and initial conditions satisfy

$$\begin{aligned} t = 0: \quad & u = 1 \quad \text{for } 0 \le x \le 1/11 \text{ and } 0 \le y \le 1/11, \\ & u = 0 \quad \text{elsewhere,} \\ t > 0: \quad & u = 1 \quad \text{for } x = 0 \text{ and } 0 \le y \le 1/11, \text{ and for } y = 0 \text{ and } 0 \le x \le 1/11, \\ & \frac{\partial u}{\partial n}\Big|_{\partial\Omega} = 0, \quad \text{elsewhere.} \end{aligned}$$

With these choices, the solution is a front that, starting as a small-sized block near (0,0), moves approximately with speed $|\beta|$ and direction β. After having reached the boundary, the solution u tends to a constant steady-state value of 1 for $t\to\infty$, as we have Neumann conditions on the remaining part of the boundary. Note, that this part of the computation is difficult, since the solution at the boundary is lifted from 0 to 1, while still obeying the Neumann conditions.

In Table 3.4 the time-integration history is presented for $\varepsilon=1.E-2$. Figure 3.3 shows the grids and solutions at t=0.3, which is halfway the propagation phase of the front. Using the standard values $\varepsilon_1^2=1.E-4$, $\varepsilon_2^2=1.E-9$ and $TOL=1.E-3$, MFE is applied to this test problem on a starting grid of 25×25 grid points, of which 13×13 are distributed uniformly over the block, and the remaining ones uniformly over the rest of the domain.

There are some interesting remarks to be made regarding the figures in the table. At first, we see a start-up phase, in which MFE tries to cope with the initial discontinuity u and the initial nonuniform grid. After that, the propagation phase of the solution dominates the performance of the moving-grid method. This can be seen from the almost constant time-integration between t=0.25 and t=0.75. In this phase, MFE approximates a perturbed characteristic movement (see (3.7)), with a small perturbation term $\varepsilon\,\mathbf{f}$. Around t=1.0 the front hits the boundary, at which point the perturbation $\mathbf{f}$ is no longer negligible. As indicated above, this part of the computation combined with the approach to steady-state takes many time steps. It must be noted, that, when taking a smaller diffusion coefficient, these effects appear even stronger. For $\varepsilon=1.E-3$, the propagation phase until t=0.75 takes only *STEPS*=41, *JACS*=24 and *BS*=142, letting the characteristic movement of the grid points show better. On the other hand, the steady-state phase becomes proportionally more expensive. Until t=100.0, the diffusion takes over the integration process: *STEPS*=333, *JACS*=212 and *BS*=1031.

t =	*STEPS*	*JACS*	*BS*	*PHASE*
0.25	32	20	106	START-UP
0.50	45	25	149	PROPAGATION
0.75	57	34	200	PROPAGATION
1.00	64	37	222	BOUNDARY EFFECTS
100.00	119	64	381	STEADY-STATE

TABLE 3.4 Example III: Integration history for $\varepsilon=10^{-2}$.

3.4. Application to a real-life problem

EXAMPLE IV ('Brine transport in a porous medium'):

This problem stems from hydrology and models the transport of salt in a porous medium [15]. In the present application we consider a particular model for isothermal, single-phase (only fluids), two component (water and salt) saturated flow, which is constituted by a system of two PDEs basic to groundwater flow: a continuity equation for the brine mass and a transport equation for the salt mass concentration. These equations are supplemented with two basic laws, viz. Darcy's law and Fick's law. After a few simplifications (see [33, 38]), the following system of two nonlinear PDEs determines the model

$$n\rho\frac{\partial\omega}{\partial t} = -\nabla\cdot(\rho\mathbf{J}) - \rho\mathbf{q}\cdot\nabla\omega \ , \tag{3.8a}$$

$$\beta n\rho\frac{\partial P}{\partial t} + \gamma n\rho\frac{\partial\omega}{\partial t} = -\nabla\cdot(\rho\mathbf{q}) \ , \tag{3.8b}$$

where

$$\mathbf{q} = -\frac{K}{\mu}(\nabla P - \rho\mathbf{g}) \quad \text{(Darcy's law)}, \tag{3.9a}$$

$$\mathbf{J} = -D\nabla\omega \quad \text{(Fick's law)}. \tag{3.9b}$$

The 2x2 dispersion tensor is defined by

$$D = (nD_{mol}+\alpha_T|\mathbf{q}|)I + \frac{\alpha_L-\alpha_T}{|\mathbf{q}|}\mathbf{q}\mathbf{q}^T, \quad |\mathbf{q}| = (\mathbf{q}^T\mathbf{q})^{1/2}, \tag{3.9c}$$

To complete the physical model, an equation of state is added, given by

$$\rho = \rho_0 e^{\beta(P-P_0)+\gamma\omega} \ . \tag{3.9d}$$

In equations (3.8) and (3.9), the following notation is used: the quantities ω, P, ρ, n, μ, K, $\mathbf{q}$, $\mathbf{J}$ and $\mathbf{g}$ represent, respectively, salt mass fraction, pressure, density, porosity, viscosity, permeability, Darcy velocity, dispersive flux and the gravity vector. Further, D_{mol} stands for the molecular diffusion, α_T for the transversal dispersion coefficient, α_L for the longitudinal dispersion coefficient, β for the compressibility, γ for a salt coefficient, and ρ_0, P_0 for reference density and pressure values.

The dispersion coefficients α_T and α_L highly determine the character of equation (3.8a). Equation (3.8a) is of the convection-diffusion (advection-dispersion) type and, as usual, numerically difficult to solve if it is

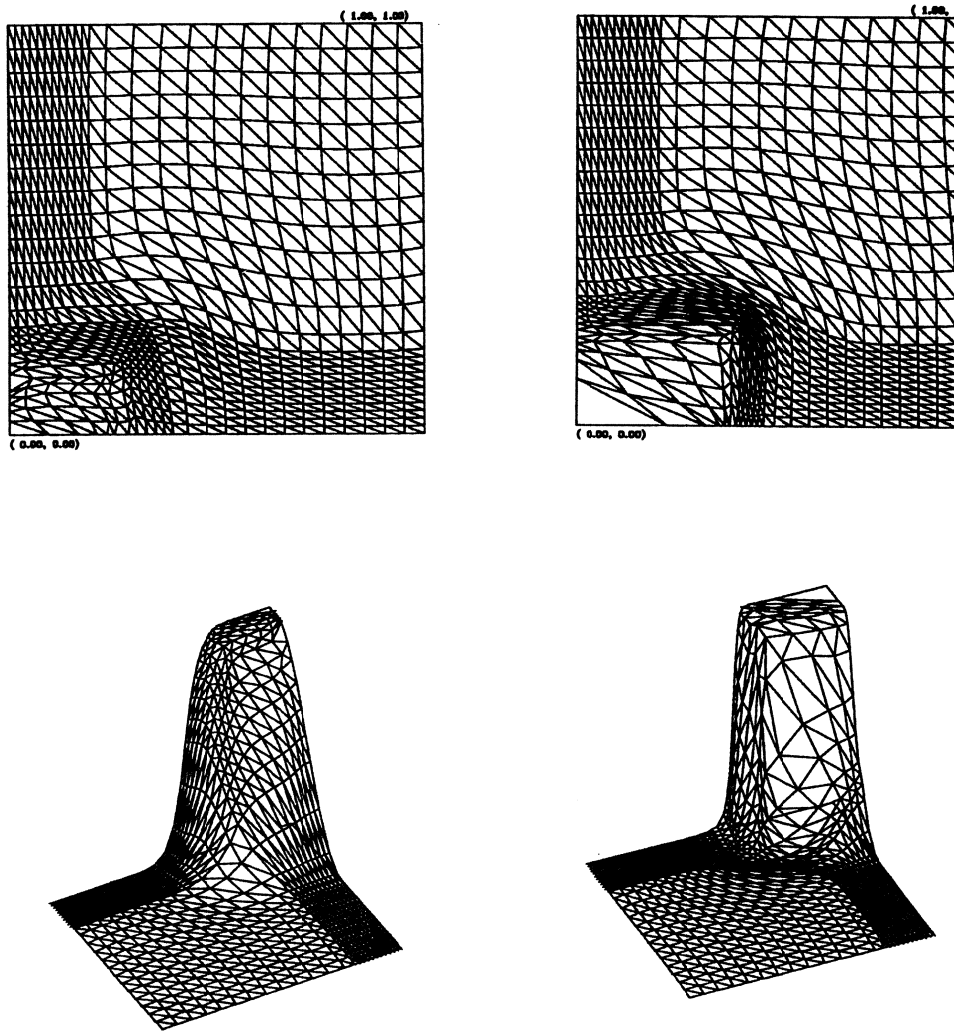

FIGURE 3.3. Grids and solutions of Example III at t=0.3 for $\varepsilon = 10^{-2}$ (left), 10^{-3}(right).

advection dominated. With the below selected initial and boundary conditions and the actual choice for α_T and α_L, steep travelling salt fronts are generated. Further, a special feature of the model is that the compressibility coefficient β is very small or even zero. If β=0, then the 2×2-matrix multiplying the time-derivative vector $(\omega_t, P_t)^T$ is singular and (3.8b) is effectively replaced by an equation without temporal derivatives. As we will use a stiff (implicit) ODE/DAE solver, viz. the BDF module of the SPRINT package, there is no need to distinguish between β=0 and $\beta \neq 0$. Finally, it is known, that the pressure equation (3.8b), can, in certain circumstances, be approximated in a so-called Boussinesq sense, replacing it by the standard continuity equation $\nabla \cdot \mathbf{q} = 0$. With the present conditions this results in a very smoothly varying pressure distribution $P(x,y,t)$. For more information with regard to the PDE model, the interested reader is referred to [33, 38].

The application of MFE to this model needs an extra explanation. There are three additional aspects worth

mentioning:

1) The first aspect is the appearance of a matrix, not equal to the identity matrix, in front of the time-derivative. However, for this, only a minor modification is needed to apply the minimization procedure, which was explained in Section 2.1. No special difficulties are encountered when working out the innerproducts for the new semi-discrete formulation.

2) The second aspect deals with the treatment of general second-order operators. This has already been treated in Section 2.2.

3) The third new aspect in this MFE-application is the use of the weight factors w_j (see equations (2.6)). The w_j were introduced to make it possible to let the grid movement equations (2.6b) and (2.6c) be dominated by certain PDE components. In the brine transport equation this possibility is very welcome. Since the pressure gradients $\partial P/\partial x$ and $\partial P/\partial y$ are expected to vary only slowly, the weight factor w_2 is taken zero. This means, that pressure effects are not taken into account in the moving-grid equations (2.6b) and (2.6c), and that the salt concentration changes take the responsibility for the grid movement (w_1=1).

In the present MFE-application constant values are taken for the permeability (K=1.E−10), viscosity (μ=1.E−3), porosity (n=0.4) and the molecular diffusion (D_{mol}=0). Further, the model is subjected to initial and boundary conditions on the unit square (0,1)×(0,1):

$$\omega(x,y,0) = 0, \qquad P(x,y,0) = p_0 - p_1 y,$$

$$y = 0 \text{ and } 2/11 < x < 8/11 \quad : \quad \partial\omega/\partial n = 0, \quad P = p_0,$$

$$y = 0 \text{ and } x \text{ elsewhere} \quad : \quad \omega = \omega_0, \quad P = p_0,$$

$$x = 0,\ 1 \text{ and } 0 < y < 1 \quad : \quad \partial\omega/\partial n = \partial P/\partial n = 0,$$

$$y = 1 \text{ and } 0 < x < 1 \quad : \quad \partial\omega/\partial n = 0, \quad P = p_0 - p_1,$$

where ω_0, p_0 and p_1 are constants: ω_0=0.25, p_0=1.7E+5, p_1=0.7E+5. The remaining problem data are: β=4.5E−10, γ=0.6923, ρ_0=9.98E+2, P_0=1.E+5 and $\mathbf{g}$=(0,−9.81)^T. The dispersion coefficients are chosen: α_T=2.E−3 and α_L=1.E−2.

Under these conditions, the model describes an injection of salt water of a high concentration through two gates at the bottom of the domain. Due to the small values of α_T and α_L, and the boundary conditions imposed on the pressure component P, the solution $\omega(x,y,t)$ of the PDE model is a travelling fresh/salt water front, moving from the lower boundary to the upper boundary. After having reached that boundary, the dispersion and the Neumann boundary condition take over the process, resulting in a smoothing out of the two fronts. For t sufficiently large the fronts disappear completely which means that the whole medium is filled with the high-salt concentration fluid.

MFE is applied to this model with a starting grid of 31×21 gridpoints, of which 11 gridpoints in the y-direction are distributed uniformly between 0 and 0.1 and the remaining ones uniformly over the rest of the domain, a time-tolerance of TOL=1.E−3, and penalty parameter values ε_1^2=1.E−4, ε_2^2=1.E−8, respectively.

t =	*STEPS*	*JACS*	*BS*	*PHASE*
0.25	40	19	118	START-UP
0.50	48	23	144	PROPAGATION
1.00	59	25	174	PROPAGATION
10.00	96	44	287	BOUNDARY EFFECTS
1.E+6	146	71	423	STEADY-STATE

TABLE 3.5 Example IV: Integration history.

Figure 3.4 shows the MFE solutions for ω at some characteristic points of time. Since the solutions for p do not change dramatically, we leave them out of the discussion. We clearly see the movement of the grid points following the two salt fronts. The lower three plots picture the steady-state process, for which finally MFE renders a uniform grid. Table 3.5 gives the time-integration history belonging to this run. It is interesting to remark that the figures in Table 3.5 are almost identical to the ones in Table 3.4. The four phases described in the previous example can also be recognized in this application: (1) the start-up phase, which costs a considerable number of *STEPS* for MFE to cope with the initial solution and grid distribution, (2) the propagation phase of the fronts, with a nearly constant time behaviour, for which the characteristic movement of the grid points is responsible, (3) the phase, in which the salt front hits the boundary and (4) the steady-state phase. The last two phases account for almost 50% of the integration effort.

For practical simulations of the model there is a need for more general boundary conditions (flux-conditions) and smaller values for the dispersion coefficients. Smaller α_T and α_L have the effect to give yet steeper fronts in ω. However, to apply MFE on such cases, we need to consider a more careful treatment of the general second order flux terms (2.9), since they have a strong influence on the grid movement, especially in the steep parts of the moving front solution, and near steady-state.

4. CONCLUSIONS

As a member of the class of moving-grid methods, the moving-finite-element method (MFE) is able to accurately approximate solutions of PDE models in two space dimensions possessing steep local transitions. In this paper MFE has been applied to PDEs with a different underlying background, viz. containing convection, reaction and/or diffusion terms. In all examined cases, steep moving front solutions are satisfactorily followed by the semi-discrete moving-grid points. It must be stressed that compared with standard fixed-grid methods, a notable advantage of MFE is, that it can be used with a relatively small number of spatial grid points, when applied to PDEs with sharp transitions.

The effect of the penalty parameters on the semi-discrete ODE system depends on the PDE to be solved. The first parameter, the intratriangular viscosity constant, ε_1, has an important influence on the efficiency of the time-stepping procedure. For small values the grid movement may become irregular, whereas for slightly larger values of ε_1 it can be seen as a grid-smoothing parameter. Too large values of ε_1 yield an (unwanted) non-moving grid. The second parameter, the intratriangular spring constant, ε_2, needs only to be used for PDEs with a flat steady-state solution, and, therefore, affects the time-integration process for large points of time. Further, the steady-state 'flame front' solution strengthens the conjecture, that, for parabolic equations, MFE is closely related to equidistribution principles.

For convection-diffusion equations MFE resembles a perturbed method of characteristics. The PDE diffusion coefficient plays an important role in this respect. Since MFE uses piecewise linear basis functions, second derivative terms are not well-defined. Several regularizations are possible to treat the troublesome innerproducts. The diffusion term and, thus the choice of regularization, influences the grid movement around steep transitions, near boundary layers and also in near steady-state situations.

MFE is applied to a brine transport problem in a porous medium. The weight factors, introduced to emphasize or de-emphasize certain PDE components, are utilized to let the grid-movement of the method merely be driven by the first component, the salt mass fraction, which consists of steep moving fronts, and not by the second component, the pressure, which varies only little during the whole time-period. A special treatment, of the general flux term is carried out, using the average of the first derivatives of the solution, to cope with undefined innerproducts.

Future developments to improve the performance of MFE, could contain: (1) the use of higher order basis/testfunctions, (2) the incorporation of an initial grid procedure (see [5]), which could also be used for regridding after grid distortion, and (3) the implementation of general flux (Robin) boundary conditions. Finally, there is a need for more theoretical results with regard to moving-finite-elements in two space dimensions.

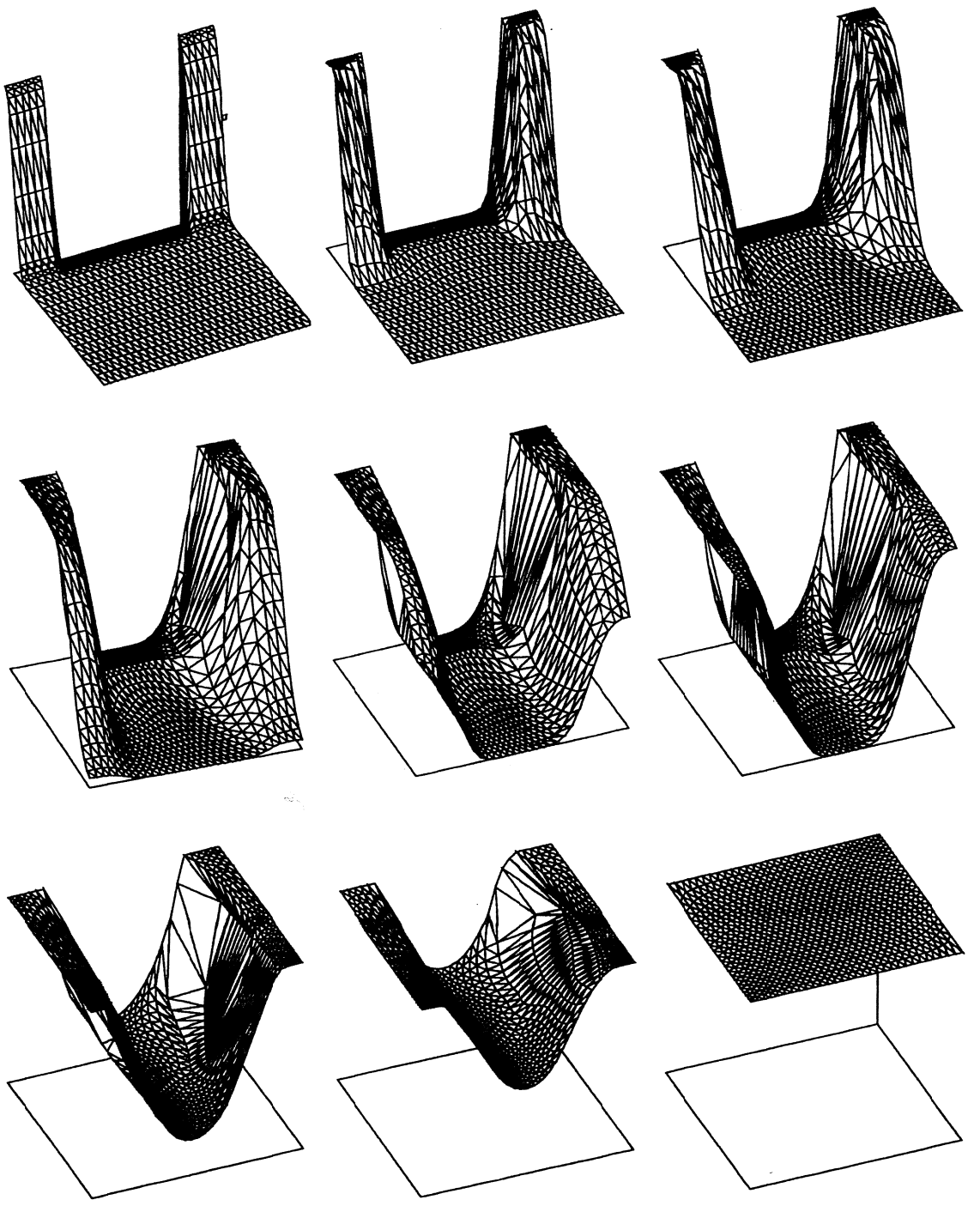

FIGURE 3.4. MFE solution of Example IV at $t = 0$, 0.1, 0.25, 0.5, 0.75, 1.0, 5.0, 10.0, $1.E+6$.

REFERENCES

1. S. ADJERID and J.E. FLAHERTY (1988). A Local Refinement Finite Element Method for Two Dimensional Parabolic Systems, *SIAM J. Sci. Stat. Comput.*, 9, 792-881.
2. R. ALEXANDER, P. MANSELLI, and K. MILLER (1979). Moving Finite Elements for the Stefan Problem in Two Dimensions, *Academia Nazionale Dei Lincei, VIII*, LXVII, 57-61.
3. R.D. ALSTEAD (1987). *Moving Finite Element Modelling of the 2D Shallow Water Equations,* Numerical Analysis Report no. 5/87, University of Reading.
4. M.J. BAINES (1991). An Analysis of the Moving Finite Element Procedure, *SIAM J. Numer. Anal.*, 28, 1323-1349.
5. M.J. BAINES (1991). Algorithms for Best Piecewise Discontinuous Linear and Constant L2 Fits to Continuous Funcions with Adjustable Nodes in One and Two Dimensions, *Preprint (submitted to SIAM J. Sci. Stat. Comput.)*, University of Reading.
6. M.J. BAINES and A.J. WATHEN (1986). Moving Finite Element Modelling of Compressible Flow, *Applied Numer. Maths.*, 2, 495-514.
7. M.J. BAINES and A.J. WATHEN (1988). Moving Finite Element Methods for Evolutionary Problems I: Theory, *J. Comput. Phys.*, 79, 245-269.
8. M. BERZINS and R.M. FURZELAND (1985). *A User's Manual for SPRINT - A Versatile Software Package for Solving Systems of Algebraic, Ordinary and Partial Differential Equations: Part 1 - Algebraic and Ordinary Differential Equations,* Report TNER.85.058, Thornton Research Centre, Shell Research Ltd., U.K..
9. M. BERZINS and R.M. FURZELAND (1986). *A User's Manual for SPRINT - A Versatile Software Package for Solving Systems of Algebraic, Ordinary and Partial Differential Equations: Part 2 - Solving Partial Differential Equations,* Report No. 202, Department of Computer Studies, The University of Leeds.
10. N. CARLSON and K. MILLER (1988). The Gradient Weighted Moving Finite Element Method in Two Dimensions, in *Finite Elements Theory and Application*, 152-164, ed. D.L. DWOYER, M.Y. HUSSAINI AND R.G. VOIGHT, Springer Verlag.
11. M.J. DJOMEHRI and K. MILLER (1981). *A Moving Finite Element Code for General Systems of PDE's in 2-D,* Report PAM-57, Center for Pure and Applied Mathematics, University of California, Berkeley.
12. J.K. DUKOWICZ (1984). A Simplified Adaptive Mesh Technique Derived from the Moving Finite Element Method, *J. Comput. Phys.*, 56, 324-342.
13. R.M. FURZELAND, J.G. VERWER, and P.A. ZEGELING (1990). A Numerical Study of Three Moving Grid Methods for One-Dimensional Partial Differential Equations which are based on the Method of Lines, *J. Comput. Phys.*, 89, 349-388.
14. R.J. GELINAS, S.K. DOSS, J.P. VAJK, J. DJOMEHRI, and K. MILLER (1983). Moving Finite Elements in 2D: Fluid Dynamics Examples, in *Scientific Computing, Ed. R. Stepleman et al.*, 29-36.
15. S.M. HASSANIZADEH, A. LEIJNSE, W.J. DE VRIES, and R.A.M. STAPPER (1990). *Experimental Study of Brine Transport in Porous Media, Intraval Test Case 13,* Reportnr. 725206003, National Institute of Public Health and Environmental Protection, Bilthoven, The Netherlands.
16. B.M. HERBST, S.W. SCHOOMBIE, and A.R. MITCHELL (1982). A Moving Petrov-Galerkin Method for Transport Equations, *Int. J. Numer. Methods Eng.*, 18, 1321-1336.
17. I.W. JOHNSON (1985). *Moving Finite Elements for Nonlinear Diffusion Problems in One and Two Dimensions,* Numerical Analysis Report no. 12/85, University of Reading.
18. I.W. JOHNSON, A.J. WATHEN, and M.J. BAINES (1988). Moving Finite Element Methods for Evolutionary Problems II: Applications, *J. Comput. Phys.*, 79, 270-297.
19. A.K. KAPILA (1983). *Asymptotic Treatment of Chemically Reacting Systems*, Pitman Advanced Publ. Company.
20. K. MILLER (1981). Moving Finite Elements II, *SIAM J. Numer. Anal.*, 18, 1033-1057.
21. K. MILLER (1983). Alternate Modes to Control the Nodes in the Moving Finite Element Method, in *Adaptive Computational Methods for PDEs*, 165-182, ed. I. BABUŠKA, J. CHANDRA AND J.E. FLAHERTY, SIAM, Philadelphia.
22. K. MILLER (1986). Recent Results on Finite Element Methods with Moving Nodes, in *Accuracy*

Estimates and Adaptive Refinements in Finite Element Computations, 325-338, ed. I. BABUŠKA, O.C. ZIENKIEWICZ, J. GAGO AND E.R. DE A. OLIVEIRA, John Wiley & Sons Ltd..

23. K. MILLER (1988). *On the Mass Matrix Spectrum Bounds of Wathen and the Local Moving Finite Elements of Baines,* Centre for Pure and Applied Mathematics report PAM-430, UCB.
24. K. MILLER and R.N. MILLER (1981). Moving Finite Elements I, *SIAM J. Numer. Anal.*, 18, 1019-1032.
25. W.J. MINKOWICZ, E.M. SPARROW, G.E. SCHNEIDER, and R.H. PLETCHER (1988). *Handbook of Numerical Heat Transfer*, John Wiley & Sons, Inc..
26. C.R. MOLENKAMP (1968). Accuracy of Finite-Difference Methods Applied to the Advection Equation, *Journal of Appl. Meteorology*, 7, 160-167.
27. P.K. MOORE and J.E. FLAHERTY (1992). Adaptive Local Overlapping Grid Methods for Parabolic Systems in Two Space Dimensions, *J. Comput. Phys.*, 98, 54-63.
28. A.C. MUELLER (1983). *Continuously Deforming Finite Element Methods for Transport Problems,* Dissertation, The Univ. of Texas at Austin.
29. A.C. MUELLER and G.F. CAREY (1985). Continuously Deforming Finite Elements, *Int. J. Numer. Methods Eng.*, 21, 2099-2126.
30. TH. L. V. STIJN, J.C.H. V. EIJKEREN, and N. PRAAGMAN (1987). *A Comparison of Numerical Methods for Air-Quality Models,* RIVM-Report 958702007, National Institute of Public Health and Environmental Protection.
31. P.K. SWEBY (1987). *Some Observations on the Moving Finite Element Method and its Implementation,* Numerical Analysis Report no. 13/87, University of Reading.
32. R.A. TROMPERT and J.G. VERWER (1991). A Static-Regridding Method for Two-Dimensional Parabolic Partial Differential Equations, *Applied Numer. Maths.*, 8, 65-90.
33. R.A. TROMPERT, J.G. VERWER, and J.G. BLOM (1992). *Application of an Adaptive-Grid Method to Brine Transport in Porous Media,* Report NM-R9201, Centre for Mathematics and Computer Science (CWI), Amsterdam (submitted to Int. J. for Numer. Meth. in Fluids).
34. J.G. VERWER, J.G. BLOM, R.M. FURZELAND, and P.A. ZEGELING (1989). A Moving-Grid Method for One-Dimensional PDEs based on the Method of Lines, in *Adaptive Methods for Partial Differential Equations*, 160-175, ed. J.E. FLAHERTY, P.J. PASLOW, M.S. SHEPHARD AND J.D. VASILAKIS, SIAM, Philadelphia.
35. A.J. WATHEN (1986). Mesh-Independent Spectra in the Moving Finite Element Equations, *SIAM J. Numer. Anal.*, 23, 797-814.
36. A.J. WATHEN and M.J. BAINES (1985). On the Structure of the Moving Finite Element Equations, *IMA J. of Numer. Anal.*, 5, 161-182.
37. P.A. ZEGELING and J.G. BLOM (1990). *A Note on the Grid Movement Induced by MFE,* Report NM-R9019, Centre for Mathematics and Computer Science (CWI), Amsterdam (to appear in Int. J. for Numer. Meth. in Eng.).
38. P.A. ZEGELING, J.G. VERWER, and J.C.H. V. EIJKEREN (1991). *Application of a Moving Grid Method to a Class of Brine Transport Problems in Porous Media,* Report NM-R9112, Centre for Mathematics and Computer Science (CWI), Amsterdam (to appear in Int. J. for Numer. Meth. in Fluids).